

PAPER • OPEN ACCESS

Thermal performance of reflective insulation system and comparison against ASHRAE Standard

To cite this article: M Z M Ashhar and C H Lim 2023 *IOP Conf. Ser.: Mater. Sci. Eng.* **1278** 012013

View the [article online](#) for updates and enhancements.

You may also like

- [Pump-turbine Rotor-Stator Interaction Induced Vibration: Problem Resolution and Experience](#)
F Zhang, PY Lowys, JB Houdeline et al.
- [Improvement in simulation of Eurasian winter climate variability with a realistic Arctic sea ice condition in an atmospheric GCM](#)
Young-Kwon Lim, Yoo-Geun Ham, Jee-Hoon Jeong et al.
- [Concurrent validity of the portable gFlight system compared to a force plate to measure jump performance variables](#)
Arran Parmar, Ashleigh Keenan and Gill Barry



244th Electrochemical Society Meeting

October 8 – 12, 2023 • Gothenburg, Sweden

50 symposia in electrochemistry & solid state science

Abstract submission deadline:
April 7, 2023

Read the call for papers &
submit your abstract!

Thermal performance of reflective insulation system and comparison against ASHRAE Standard

M Z M Ashhar and C H Lim

Solar Energy Research Institute, Universiti Kebangsaan Malaysia, 43650 Bangi,
Selangor Malaysia

chinhaw.lim@ukm.edu.my

Abstract. The trend in building energy consumption has been steadily increasing and will continue to rise significantly in the future. The application of a reflective insulation system in roof assembly is proven to be effective in reducing heat gain across the roof and can enhance indoor thermal comfort. This paper presents the development of an Indoor Solar Simulator to evaluate the thermal resistance (RSI value) of reflective insulation systems for roof assemblies. This paper also compares RSI values obtained experimentally and the RSI values listed in ASHRAE Standard. The roof assemblies studied in this paper incorporate the same reflective insulation systems as listed in ASHRAE Standard. Thermocouples and heat flux transducers are installed at various locations and the RSI values are calculated using the average method as detailed in ISO 9869-1:2014. From the error analysis, it can be concluded the RSI values obtained experimentally using the Indoor Solar Simulator and ASHRAE Standard are in a good agreement with MAPE value of 6.13%. These discrepancies could be due to the thermal bridges from mechanical supports inside the air gap, or possibly the air gaps are not completely airtight and unventilated.

1. Introduction

In 2020, the building sector accounted for 36% of global final energy consumption and 37% of energy-related carbon emissions. Although carbon emissions dropped slightly compared to the previous year due to the global pandemic, the reopening of the economic sector is expected to increase the emissions. One of the major contributions to high carbon emissions and high energy consumption in buildings is space cooling. It is responsible for 5% of total energy consumption worldwide in 2020. Furthermore, the energy use for space cooling is expected to double in 2040 [1]. This poses a huge challenge, especially for countries in the Tropics region where cooling is dominant as air-conditioning can make up to 50% of the total electricity usage [2].

All year long, Malaysia experiences hot and humid weather, which causes a tremendous amount of heat gain in buildings. High energy demand for cooling has resulted from the choice of construction materials, particularly the roof [3]. A significant portion of the solar energy entering a building is absorbed by exposed roof surfaces and transferred into the building. When compared to other building elements, the roof is the one that causes the greatest temperature variations in single-story homes or low-rise buildings [4]. According to Nahar et al. [5], the roof contributes 36.7% of the heat load in a single-story home. According to Vijaykumar et al. [6], between 50% and 70% of heat is transmitted through the roofs of single-story or double-story buildings. Conduction, convection, and radiation are how solar heat enters a structure. Radiation accounts for about 87% of the total heat energy that enters



the building through the roof, with conduction and convection heat transfer providing the balance [7]. Concrete tiles, clay tiles, and metal decks are a few of the often-used roofing materials in Malaysian homes. These roofing materials allow a lot of solar heat into buildings, raising interior temperatures, using more energy, and making indoor spaces uncomfortable [8].

1.1. Reflective insulation system

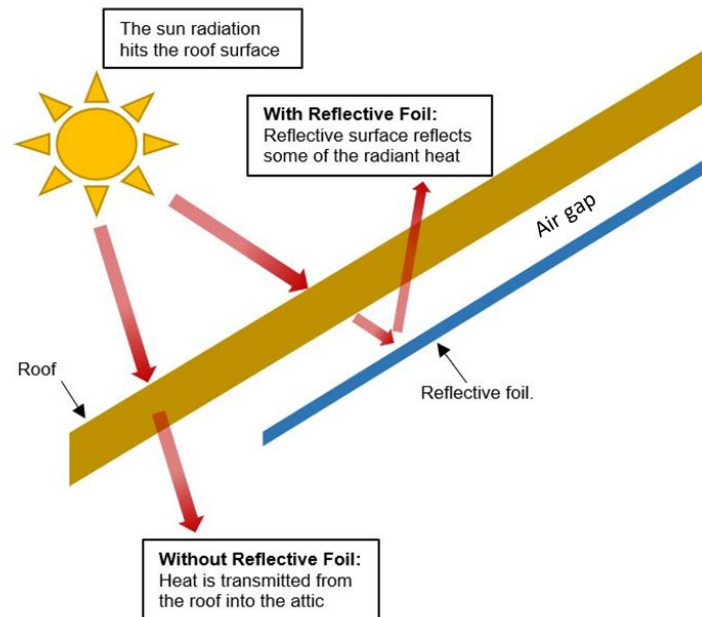


Figure 1. Working principle of reflective insulation system in a roof system [10]

According to Reflective Insulation Manufacturers Association International or RIMA-I, a reflective insulation system is when a reflective foil with a low emissivity characteristic on one or both sides of the foil, is installed adjacent to an air gap. The low emissivity side of the foil ($\epsilon = 0.01 - 0.05$) must be installed adjacent to an air gap for the system to reflect radiant heat transfer effectively as shown in Figure 1. However, the opposite effect is observed if the reflective foil is stacked between two solid materials, as the conductive heat transfer will be high. Based on the previous literature, there are various factors affecting the performance of a reflective insulation system as a roof insulation, such as the emissivity value, thickness of the air gap, air gap ventilation, roof pitch, dusting effect, weather, and climatic conditions [10].

1.2. Previous work

The use of an indoor solar simulator to investigate roof thermal performance has been utilised by previous researchers. Researchers favoured this method as it allows the research to be conducted in a steady-state environment and the modifications to the roof assembly can be done immediately. It was proven that an indoor solar simulator can produce a reliable and accurate measurement in evaluating roof thermal performance.

There were some similarities and differences between the previous indoor solar simulators. In terms of the choice of the light source, Chang et al. [11] used halogen light bulbs, whereas Roels & Deurinck [12] used infrared light bulbs to generate solar irradiance of 600 W/m^2 . In contrast, Shrestha

et al. [13] heated the roof surface and maintained it at 60°C using infrared light bulbs to simulate summer conditions. One significant benefit of using an indoor solar simulator is the ease of changing the roof configurations and test parameters. For example, Roels & Deurinck [12] and Shrestha et al. [13] were able to change the type of radiant barrier, whereas Chang et al. [11] were able to change the position of the radiant barrier. Most importantly, steady-state measurements can be obtained as the research is conducted in a controlled indoor environment which is vital to obtain consistent results and not influenced by the transient outdoor environment. Although previous research has shown that steady-state measurements can be obtained via indoor laboratory experiments, none of the past research has made a comparison or validation against ASHRAE Standard.

1.3 RSI values of enclosed air gaps as listed in the ASHRAE Standard

Previously, The American Society of Heating, Refrigerating, and Air-Conditioning Engineers (ASHRAE) has provided the RSI values of reflective insulation systems (enclosed air gaps facing a low emissivity surface). The RSI values of enclosed reflective air gaps are based on the reduced radiative transport across the air gaps and convection/conduction occurring in the air gap, so air film resistances are included. Table 2 below shows the RSI values of enclosed air gaps facing surfaces of different emissivity ($\epsilon = 0.03, 0.05, 0.2, 0.5, 0.82$) and air gap thicknesses from 12.7 mm to 139.7 mm. The angle of the enclosed air gap is kept at 0° (horizontal plane), and the heat direction is downwards from top to bottom surface.

Table 1. The RSI values of enclosed air gaps listed in the ASHRAE Standard [14]

Air gap thickness (mm)	RSI value (m ² K/W)				
	$\epsilon = 0.03$	$\epsilon = 0.05$	$\epsilon = 0.2$	$\epsilon = 0.5$	$\epsilon = 0.82$
12.7	0.437	0.412	0.294	0.187	0.136
19	0.625	0.579	0.370	0.215	0.150
38	1.073	0.942	0.491	0.252	0.166
88.9	1.774	1.442	0.601	0.277	0.176
139.7	2.064	1.627	0.631	0.284	0.178

1.4 Research objective

This paper presents the development of an indoor solar simulator to investigate the thermal resistance (RSI values) of reflective insulation systems for roof applications. This research focuses on validating the Indoor Solar Simulator test results and comparison with RSI values of enclosed air gaps presented in the ASHRAE Standard.

2. Details of the indoor solar simulator for the roof thermal resistance measurement

For this research, an indoor solar simulator was built in Universiti Kebangsaan Malaysia in Selangor, Malaysia (latitude 2°55'16.4"N and longitude 101°46'15.6"E). According to the Koppen-Geiger climate classification, the climate in Malaysia is categorised as Tropical Rainforest. Malaysia has a maximum temperature between 29°C and 30.3°C and high relative humidity between 82% and 90% annually. Besides that, Malaysia also suffers from a lot of rain even during the driest month with an annual rainfall of 2981 mm [15].

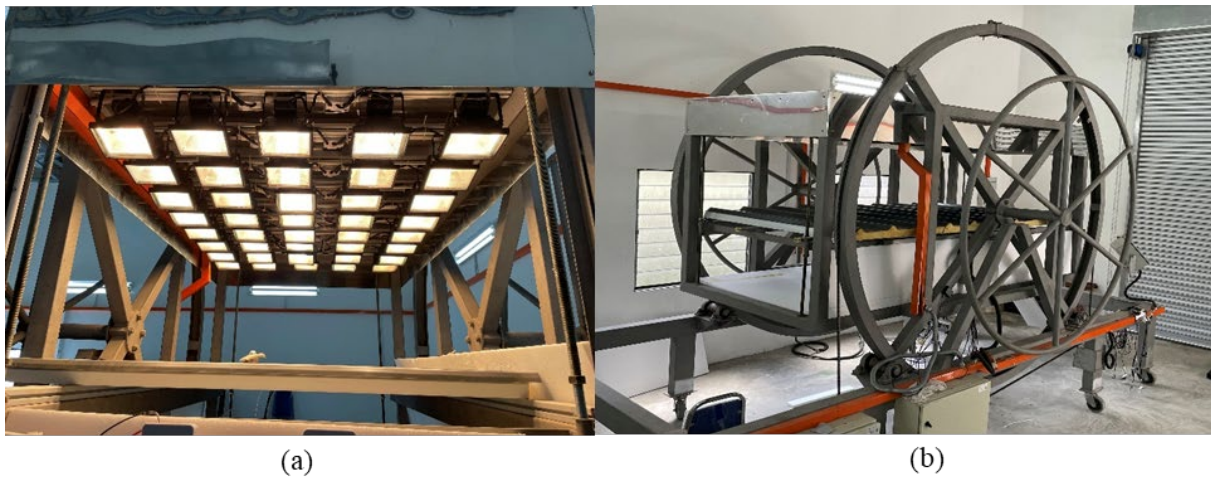


Figure 2. (a) Halogen lamps used to roof surface (b) The overall view of the indoor solar simulator

The indoor solar simulator aims to evaluate the RSI value of various types of roof configurations under hot and humid conditions. The indoor solar simulator was designed in such a way that the roof can be assembled and disassembled easily so that various designs of roof configurations can be installed and measured conveniently. The indoor solar simulator is exposed to a steady-state indoor environment with an average indoor temperature of 31°C and 80% relative humidity. The wind effect is assumed to be negligible as there is minimal air movement inside the building. The steady-state indoor conditions ensure more accurate and repeatable measurements, with a shorter time taken to complete each measurement.

2.1. Sensors and data acquisition system

To analyse the thermal response of the roof assembly, three pieces of thermocouples are positioned on the outer roof surface (T_{1A} , T_{1B} , T_{1C}) and three pieces of thermocouples are positioned on the inner roof surface (T_{2A} , T_{2B} , and T_{2C}). Two pieces of heat flux transducers are placed on the inner roof surface (q_1 and q_2). The signals transmitted by the sensors are logged at the one-minute interval by the Arduino controller and data acquisition system. Each sensor has been calibrated within the previous 24 months. The roof inclination angle can be varied from 0° (horizontal) to 90° (vertical). The test specimen size is 1.5 m in width and 3 m in length. Figure 3 shows the test setup and the positions of the sensors.

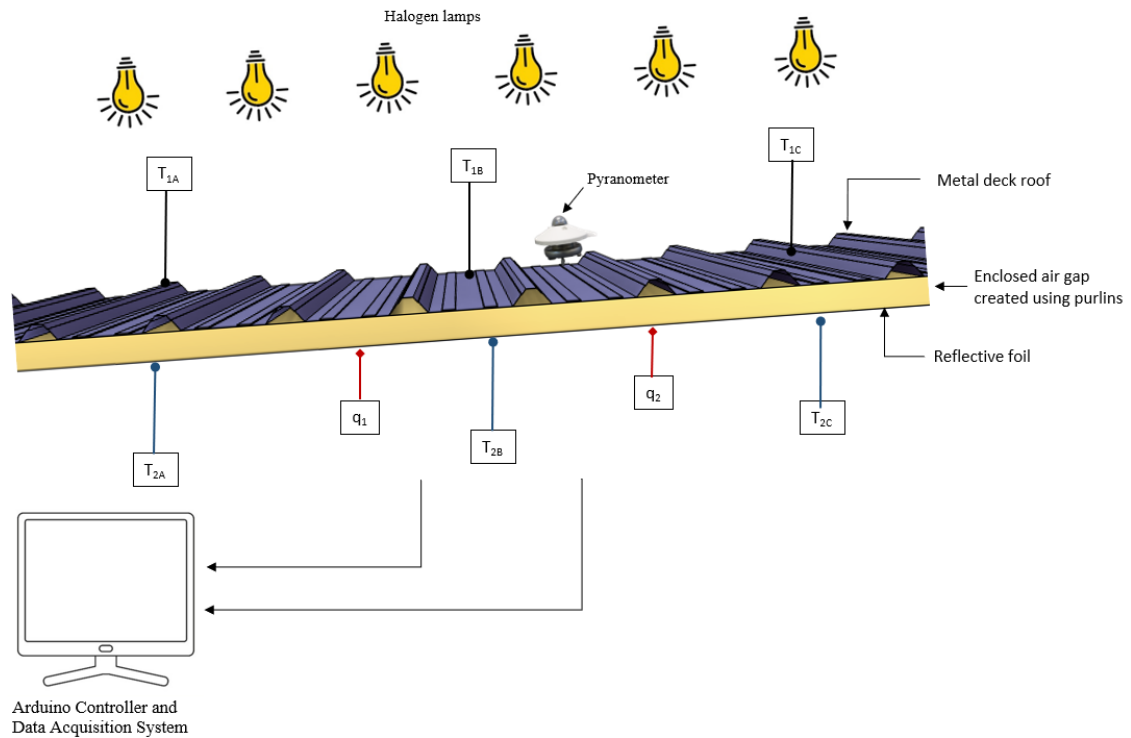


Figure 3. Positions of the thermocouples and heat flux transducers on the test assembly

3. Methodology

3.1. Validation of roof surface temperature against outdoor measurement

To ensure a realistic experiment is conducted, the indoor solar simulator measurement of roof surface temperature was first validated against outdoor measurement. The outdoor heat flux measurement is nearly impossible to obtain due to the unsteady-state condition of the outdoor environment. The roof assembly used for validation is a Metal deck roof with polyurethane (PU) insulation.

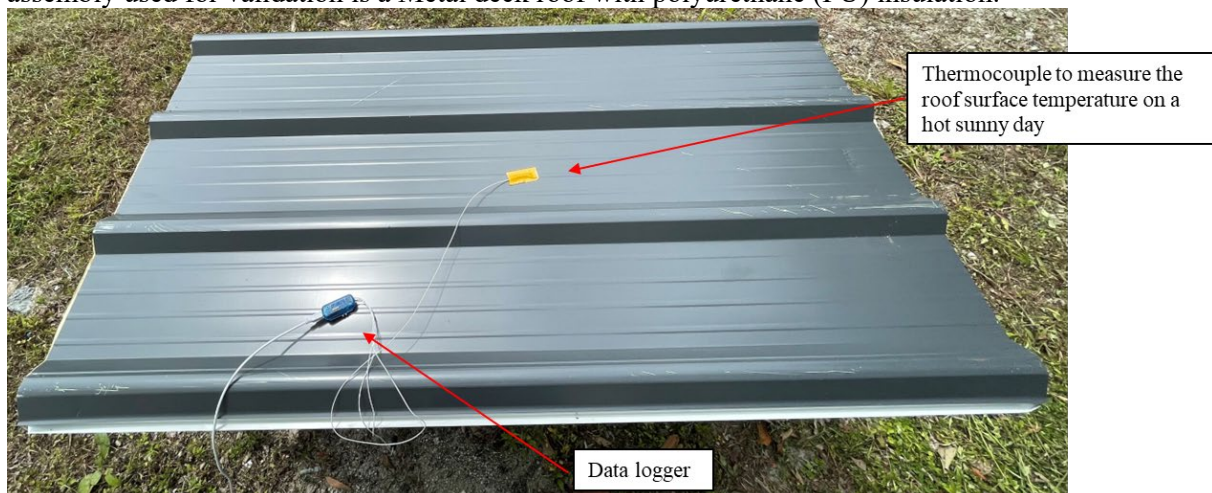


Figure 4. Measuring the roof surface temperature of a metal deck roof on a hot sunny day in Malaysia

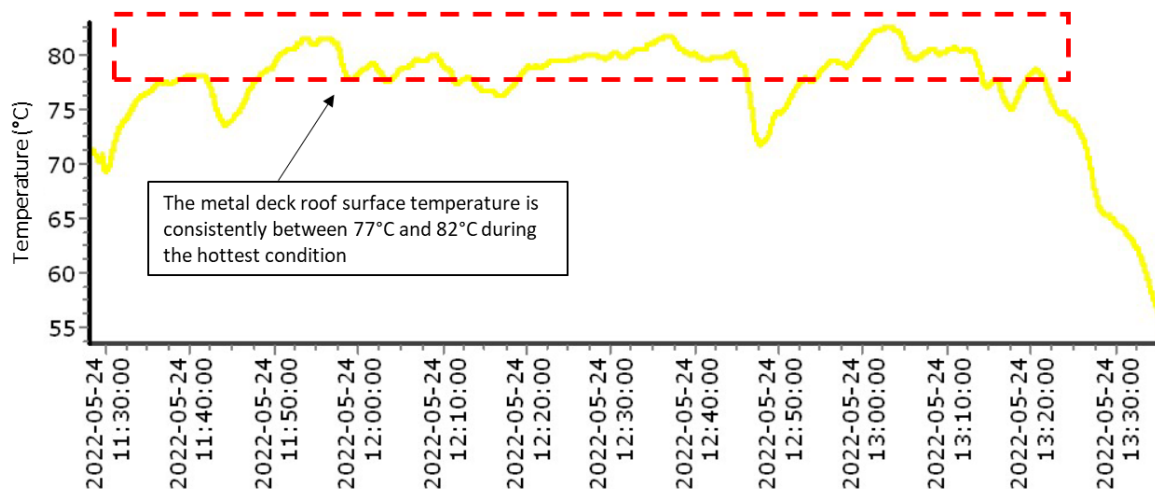


Figure 5. Roof surface temperature of metal deck roof at an outdoor condition during the hottest condition of a sunny day in Malaysia

The outdoor surface temperature of the metal deck roof with PU insulation was taken during the daytime. It was found that the maximum outdoor surface temperature reaches a maximum constant temperature of 77°C – 82°C in the afternoon. For the indoor solar simulator measurement, the power supplied to the halogen lamps is adjusted so that the outer roof surface temperature of the metal deck roof with PU insulation reaches a constant temperature of 77°C – 82°C, mirroring the values obtained from the outdoor measurement. The same amount of power supply is applied for all measurements using the indoor solar simulator.

3.2. Data collection

The desired roof configuration is assembled on the indoor solar simulator. After the halogen lamps are turned on, the roof surface temperature and heat flux readings are constantly monitored and recorded every 2 seconds. The readings typically reach a steady-state condition 1 hour after the lamps are turned on. The measurement is continued for an extra 3 hours after the steady-state condition was achieved to ensure a stable and accurate reading is obtained. The roof surface temperatures (T_{1A} , T_{1B} , T_{1C} , T_{2A} , T_{2B} , and T_{2C}), and heat flux transmissions (q_1 and q_2) in the steady-state period are extracted to calculate the RSI value of the entire roof assembly.

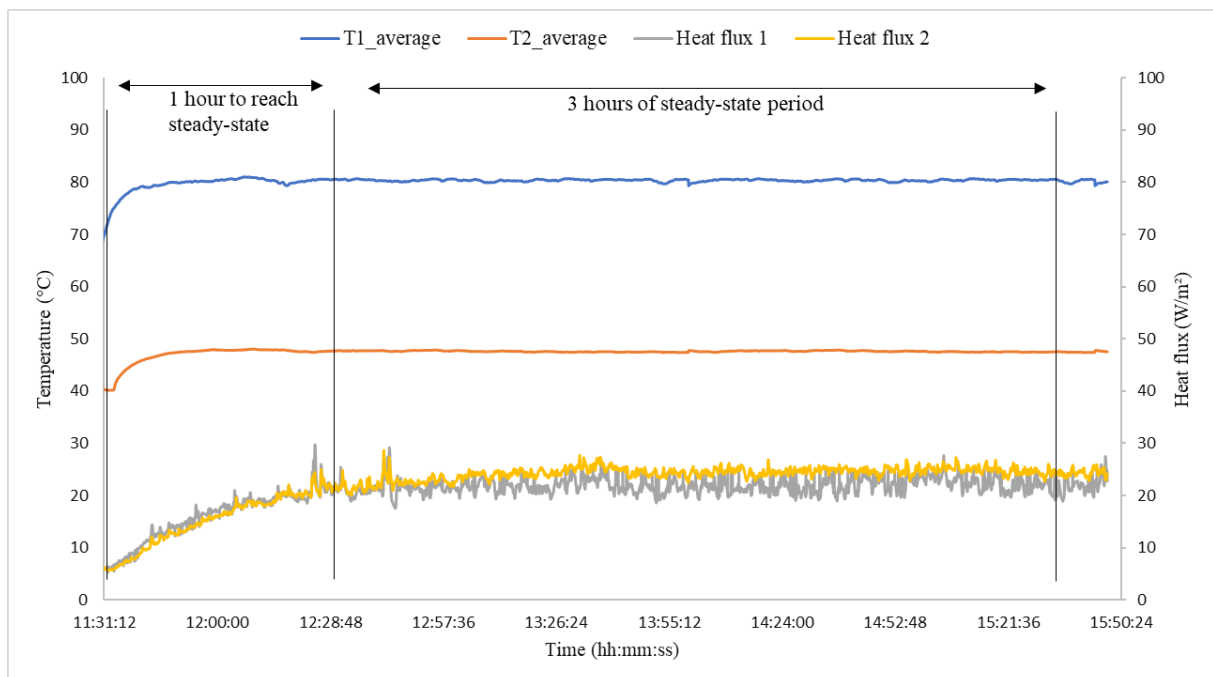


Figure 6. Measurement of roof surface temperature and heat flux penetration using the indoor solar simulator. A Steady state is achieved 1 hour after measurement starts.

3.3. Thermal Resistance (RSI value) calculation method

The method chosen to determine the RSI value of the entire roof assembly is the average method as detailed in ISO 9869-1:2014. The calculation is achieved by summing up the average temperature differences between the outer roof surface and inner roof surface ($T_{1_avg} - T_{2_avg}$) and dividing them by the sum of all averaged heat fluxes (q_{avg}). The surface temperature and heat flux values used for the RSI value calculation are the values in the steady-state period. This step is repeated for all roof configurations studied in this research.

$$RSI = \frac{\sum(T_{1_avg} - T_{2_avg})}{\sum(q_{avg})} \quad (1)$$

where:

T_{1_avg} = Average values of T_{1A} , T_{1B} , and T_{1C}

T_{2_avg} = Average values of T_{2A} , T_{2B} , and T_{2C}

q_{avg} = Average values of q_1 and q_2

3.4. Specification of the roof configurations in this study

The roof configurations in this study are aimed to mimic the assembly as reported by ASHRAE Standard. Therefore, the reflective insulation systems are made up of metal deck shingles with a reflective foil ($\epsilon = 0.03$) separated by an enclosed air gap created using purlins. The reflective foil's low emissivity side faces the enclosed air gap (upwards) for all roof configurations. The thicknesses of enclosed air gaps are 25 mm, 50 mm, 75 mm, 100 mm, and 125 mm. The roof pitch of all roof configurations is maintained at 0° (horizontal).

Table 2. Illustration and description of the studied roof configurations

Number	Illustration of the roof configuration	Description
1		<ol style="list-style-type: none"> 1. Metal deck roof 2. Air gap 25 mm 3. Reflective foil ($\epsilon = 0.03$)
2		<ol style="list-style-type: none"> 1. Metal deck roof 2. Air gap 50 mm 3. Reflective foil ($\epsilon = 0.03$)
3		<ol style="list-style-type: none"> 1. Metal deck roof 2. Air gap 75 mm 3. Reflective foil ($\epsilon = 0.03$)
4		<ol style="list-style-type: none"> 1. Metal deck roof 2. Air gap 100 mm 3. Reflective foil ($\epsilon = 0.03$)
5		<ol style="list-style-type: none"> 1. Metal deck roof 2. Air gap 125 mm 3. Reflective foil ($\epsilon = 0.03$)

4. Results and Discussions

Figure 8 below shows the RSI values of roof assembly obtained experimentally against ASHRAE Standard for various air gap thicknesses. The ASHRAE Standard values are shown in Table 2 ($\epsilon = 0.03$). It can be seen that the RSI values obtained experimentally are always higher than ASHRAE Standard for all air gap thicknesses despite both plots having similar trends.

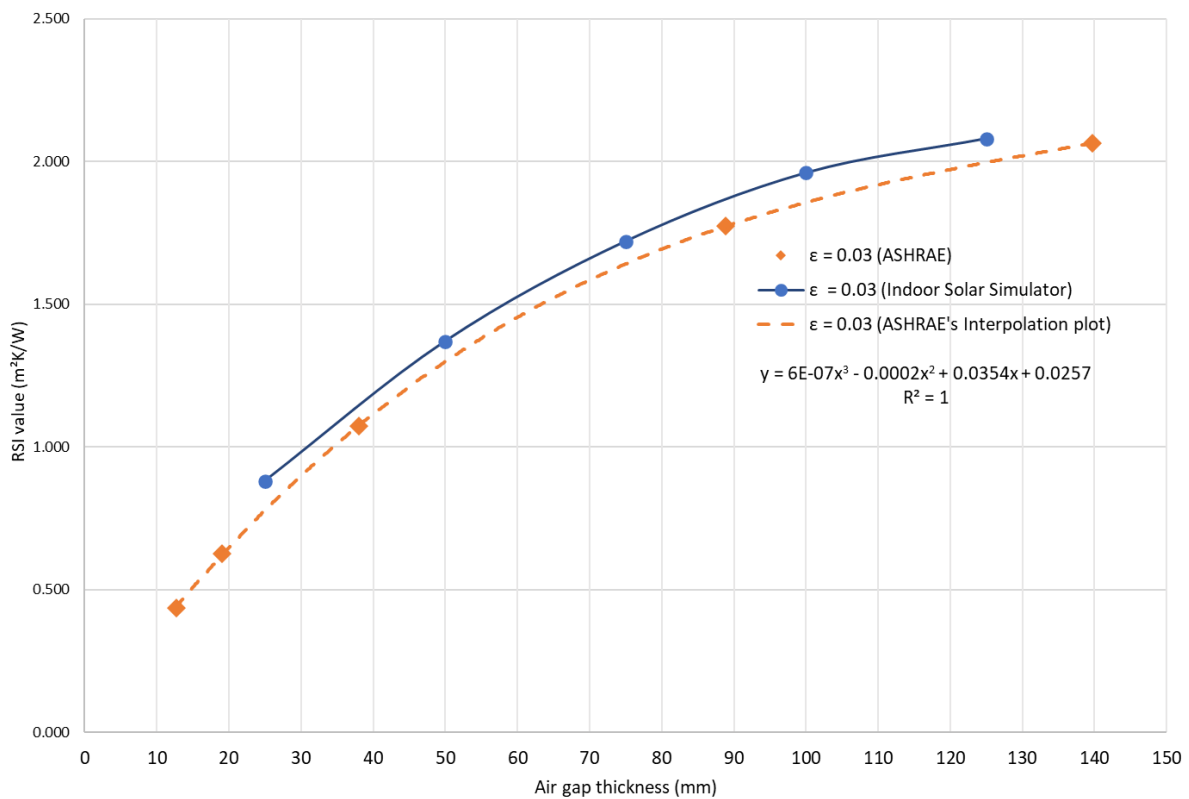


Figure 7. RSI values of roof assembly obtained from the Indoor Solar Simulator and ASHRAE Standard

Table 3. The percentage error of RSI values obtained from the Indoor Solar Simulator and ASHRAE Standard

Air gap thickness (mm)	RSI value from ASHRAE's Interpolation (m²K/W)	RSI value from Indoor Solar Simulator(m²K/W)	Percentage error (%)
25	0.78	0.88	11.60
50	1.30	1.37	5.17
75	1.64	1.72	4.58
100	1.86	1.96	5.29
125	2.00	2.08	4.03
Mean absolute percentage error (MAPE)			6.13

Table 7 shows the percentage error of RSI values between the Indoor Solar Simulator and the ASHRAE Standard. As the air gap thicknesses listed in ASHRAE Standard (as shown in Table 2) and the air gaps evaluated using Indoor Solar Simulator are not the same, hence an interpolation plot was used to estimate the ASHRAE's RSI values roof assemblies with air gap thickness of 25 mm, 50 mm,

75 mm, 100 mm, and 125 mm. The percentage error is about 4% - 5% for air gap thickness between 50 mm and 125 mm. For the air gap of 25 mm, however, the percentage is quite high at 11.60%. From the error analysis, it can be concluded the RSI values obtained experimentally using the Indoor Solar Simulator and ASHRAE Standard are in a good agreement with MAPE value of 6.13%.

The RSI values in ASHRAE Standard are obtained for ideal conditions with simplified assumptions such as disregarding any thermal bridges from mechanical supports inside the air gap, and the air gaps are completely airtight and unventilated [16]. These conditions are almost impossible to achieve in an experimental condition and which justifies the errors obtained experimentally using the Indoor Solar Simulator.

5. Conclusion

The paper presents the development of an indoor solar simulator for evaluating the roof's thermal performance in terms of RSI value and comparison against the RSI values listed in the ASHRAE Standard. Halogen light bulbs are used to simulate sun radiation which is directed toward the outer roof surface. Thermocouples are installed on the outer and inner roof surfaces, and heat flux sensors are installed on the inner surface. The surface temperature of various roof surfaces and heat flux transmissions are recorded 3 hours after steady-state conditions are achieved. RSI values are calculated using the average method as detailed in ISO 9869-1:2014. The error analysis showed that the RSI values obtained experimentally and in ASHRAE Standard are in good agreement with MAPE value of 6.13%. Several reasons for the errors are because of thermal bridges in the air gaps, which occur in the experimental roof assembly, and lack of airtightness which causes the air inside the air gap to be ventilated. As the workmanship of the roof assembly can affect the accuracy of the measurements, the researchers must ensure the roofs are assembled properly, and the air gaps are always airtight and unventilated.

6. References

- [1] United Nations, "Global Status report for Buildings and Construction 2021," *United Nations Environ. Program.*, 2021, [Online]. Available: <https://globalabc.org/resources/publications/2021-global-status-report-buildings-and-construction>.
- [2] International Energy Agency (IEA), "'The Future of Cooling Opportunities for energy-efficient air conditioning' International Energy Agency Website: www.iea.org, 2018," 2018, [Online]. Available: www.iea.org.
- [3] A. M. Abdul Rahman, N. M. S. @ Abd.Rahim, K. Al-Obaidi, M. Ismail, and L. Yoke Mui, "Rethinking the Malaysian Affordable Housing Design Typology in View of Global Warming Considerations," *J. Sustain. Dev.*, vol. 6, no. 7, pp. 134–146, 2013, doi: 10.5539/jsd.v6n7p134.
- [4] I. Hernández-Pérez, G. Álvarez, J. Xamán, I. Zavala-Guillén, J. Arce, and E. Simá, "Thermal performance of reflective materials applied to exterior building components - A review," *Energy Build.*, vol. 80, pp. 81–105, 2014, doi: 10.1016/j.enbuild.2014.05.008.
- [5] Nahar N, Sharma P, and P. M., "Performance of Different Passive Techniques for Cooling of Buildings in Arid Regions," *Build. Environ.*, vol. 38, no. 1, pp. 109–116, 2003, doi: 10.1016/S0360-1323(02)00029-X.
- [6] K. C. K. Vijaykumar, P. S. S. Srinivasan, and S. Dhandapani, "A performance of hollow clay tile (HCT) laid reinforced cement concrete (RCC) roof for tropical summer climates," *Energy Build.*, vol. 39, no. 8, pp. 886–892, 2007, doi: 10.1016/j.enbuild.2006.05.009.
- [7] F. Richards and D. Hassal, *Reflective Insulation and the Control of Thermal Environments*, Metric edi. Sydney, Australia, 1977.
- [8] K. M. . Al-Obaidi, M. Ismail, and A. M. Abdul Rahman, "Passive cooling techniques through reflective and radiative roofs in tropical houses in Southeast Asia: A literature review," *Front.*

- Archit. Res.*, vol. 3, no. 3, pp. 283–297, 2014, doi: 10.1016/j.foar.2014.06.002.
- [9] Department of Standards Malaysia, *Energy efficiency and use of renewable energy for non-residential buildings - Code of practice (MS 1525:2014)*. 2014.
- [10] M. Z. Mohd Ashhar and L. C. Haw, “Recent research and development on the use of reflective technology in buildings – A review,” *J. Build. Eng.*, vol. 45, no. October 2021, p. 103552, 2021, doi: 10.1016/j.jobbe.2021.103552.
- [11] P. C. Chang, C. M. Chiang, and C. M. Lai, “Development and preliminary evaluation of double roof prototypes incorporating RBS (radiant barrier system),” *Energy Build.*, vol. 40, no. 2, pp. 140–147, 2008, doi: 10.1016/j.enbuild.2007.01.021.
- [12] S. Roels and M. Deurinck, “The effect of a reflective underlay on the global thermal behaviour of pitched roofs,” *Build. Environ.*, vol. 46, no. 1, pp. 134–143, 2011, doi: 10.1016/j.buildenv.2010.07.005.
- [13] S. Shrestha, W. Miller, and A. Desjarlais, “Thermal Performance Evaluation of Attic Radiant Barrier Systems Using the Large Scale Climate Simulator (LSCS),” *ASHRAE Trans.*, 2013.
- [14] ASHRAE, “Chap. 26: Heat, air and moisture control in building assemblies - Material properties,” in *ASHRAE Handbook of Fundamentals*, 2009, pp. 26.1--26.22.
- [15] Climate-Data, “Climate: KUALA LUMPUR,” 2021. <https://en.climate-data.org/asia/malaysia/kuala-lumpur/kuala-lumpur-715107/>.
- [16] A. Pourghorban and B. M. Kari, “Evaluation of reflective insulation systems in wall application by guarded hot box apparatus, and comparative investigation with ASHRAE and ISO 15099,” *Constr. Build. Mater.*, vol. 207, pp. 84–97, 2019, doi: 10.1016/j.conbuildmat.2019.02.097.